

# Structures and Kinetic Stabilities of the Possible Complexes of Mononuclear Ni and (N<sub>2</sub>)<sub>x</sub> (x = 1–4)

Jun Guan<sup>\*,†</sup> and Qianshu Li<sup>‡</sup>

The School of Pharmacology, Beijing University of Chinese Medicine and Pharmacology, Beijing 100029, China, and The School of Science, Beijing Institute of Technology, Beijing 100081, China

Received: May 17, 2005; In Final Form: July 30, 2005

Ab initio and density functional theory (DFT) methods have been applied to study the structures and kinetic stabilities of the possible products of the reactions of mononuclear nickel with (N<sub>2</sub>)<sub>x</sub> (x = 1–4). Energy analyses show that end-on bound Ni(N<sub>2</sub>)<sub>x</sub> (x = 1–4) complexes are preferred to side-on and N<sub>4</sub> bound ones. Several decomposition and isomerization pathways for Ni(N<sub>2</sub>)<sub>x</sub> (x = 2–4) were investigated at the B3LYP/6-31G\* level of theory. The present study suggests that besides the four experimentally assigned complexes (NiN<sub>2</sub> (C<sub>∞v</sub>), Ni(N<sub>2</sub>)<sub>2</sub> (D<sub>∞h</sub>), Ni(N<sub>3</sub>)<sub>2</sub> (D<sub>3h</sub>), and Ni(N<sub>2</sub>)<sub>4</sub> (T<sub>d</sub>)), another two complexes (Ni(N<sub>2</sub>)<sub>4</sub> (C<sub>2v</sub>) and Ni(N<sub>2</sub>)<sub>4</sub> (D<sub>4d</sub>)) are likely to be kinetically stable, while other complexes may be kinetically unstable with barrier heights of less than 30 kcal/mol. The present study also suggests that side-on bound N<sub>2</sub> ligand is ready to transform into the end-on bound one, while N<sub>4</sub> ligand is hard to transform into side-on or end-on bound N<sub>2</sub> ligand.

## 1. Introduction

Transition metal dinitrogen complexes have received considerable attention from the interest in direct nitrogen fixation. The first prepared stable transition metal dinitrogen complex is [Ru(NH<sub>3</sub>)<sub>5</sub>N<sub>2</sub>]<sup>2+</sup>.<sup>1</sup> Following the initial work, dinitrogen complexes have been investigated for many transition metals.<sup>2–15</sup> For the nickel dinitrogen complexes, most of our knowledge comes from the experimental synthesis and spectroscopic characterization.<sup>2–4,6,8</sup> Burdett and Turner<sup>2</sup> reported preliminary infrared data for the Ni/N<sub>2</sub> reaction in low-temperature matrices, which indicates the existence of the nickel dinitrogen complexes. Subsequently, Huber and co-workers<sup>3</sup> investigated in detail the synthesis and characterization of the nickel dinitrogen complexes in low-temperature matrices. According to their investigation, four mononuclear nickel dinitrogen complexes, NiN<sub>2</sub> (C<sub>∞v</sub>), Ni(N<sub>2</sub>)<sub>2</sub> (D<sub>∞h</sub>), Ni(N<sub>3</sub>)<sub>2</sub> (D<sub>3h</sub>), and Ni(N<sub>2</sub>)<sub>4</sub> (T<sub>d</sub>), were assigned on the basis of the infrared and Raman activities. However, owing to the low absorbance, the possible ν Ni–N<sub>2</sub> stretching modes were not given for most of those assigned structures except for the Ni(N<sub>2</sub>)<sub>4</sub> (T<sub>d</sub>). In a follow-up paper, by using long matrix depositions, the low absorbance was surmounted by Klotzbücher and Ozin.<sup>4</sup>

Compared with the experimental reports on the Ni/N<sub>2</sub> system, knowledge obtained by theoretical studies is scarce. Bauschlicher et al.<sup>5</sup> previously reported an ab initio study of NiN<sub>2</sub> by using the modified coupled pair functional method (MCPF) and a short Ni–N bond length of NiN<sub>2</sub> was predicted, which stands in contradiction with the result of Klotzbücher and Ozin.<sup>4</sup> To settle that contradiction, Manceron et al.<sup>6</sup> reinvestigated the vibrational spectrum of NiN<sub>2</sub> and carried out a DFT study at the same time. In addition, Ciullo et al.<sup>7</sup> have performed full optimization on the geometries of NiN<sub>2</sub> for both side-on and end-on coordination modes at the MCPF level of theory.

Until now, there were four mononuclear nickel dinitrogen complexes that had been assigned.<sup>3</sup> Owing to the low absorbance of their vibrational frequency modes and/or the difficulty of distinguishing their vibrational frequencies from those of other's, could there exist any other possible mononuclear nickel dinitrogen complexes that have not been assigned? What will be the calculated Ni–N and N–N stretching frequencies of these complexes at the DFT level of theory? What are the thermodynamic and kinetic stabilities of these unassigned complexes? To answer these questions, the structures, energies, harmonic vibrational frequencies, and kinetic stabilities of the mononuclear Ni(N<sub>2</sub>)<sub>x</sub> (x = 1–4) complexes are investigated in the present paper.

## 2. Calculation Methods

All calculations were carried out with the Gaussian 98 program package.<sup>16</sup> The geometries of the Ni(N<sub>2</sub>)<sub>x</sub> (x = 1–4) complexes and their corresponding transition states were fully optimized at the B3LYP/6-31G\* level of theory. Harmonic vibrational frequency analyses were carried out at the same level to check whether the obtained structure is a local minimum (frequencies are all real) or a transition state (only one imaginary frequency). Then, the geometries were optimized and the harmonic vibrational frequencies were calculated at the MP2/6-31G\* level for the Ni(N<sub>2</sub>)<sub>x</sub> (x = 1–3) complexes, and at the B3LYP/6-31G\* level for the Ni(N<sub>2</sub>)<sub>x</sub> (x = 4) complexes. Further calculations for the Ni(N<sub>2</sub>)<sub>x</sub> (x = 1–4) complexes on their geometrical optimization were performed at the B3LYP/6-311+G\* level of theory. And based on the obtained geometries, calculations on the single-point energies were performed at the B3LYP/6-311+G(3df,3pd) level of theory. Intrinsic reaction coordinate (IRC) calculations were carried out at the B3LYP/6-31G\* level of theory to test whether the transition state connects the right minima. Throughout this paper, bond lengths are provided in angstroms, bond angles in degrees, total energies in hartrees, and relative energies and zero-point vibrational energies in kilocalories/mole, unless otherwise stated.

\* Address correspondence to this author. E-mail: timeguan@sina.com.

† Beijing University of Chinese Medicine and Pharmacology.

‡ Beijing Institute of Technology.

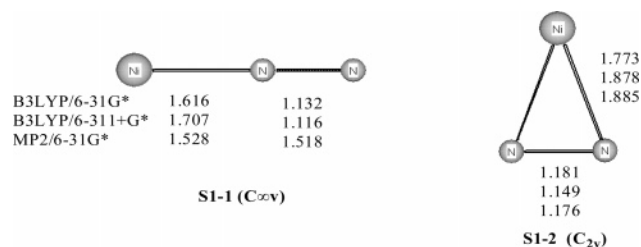


**Figure 1.** Optimized structures for **S1-1** ( $C_{2v}$ ) and **S1-2** ( $C_{2v}$ ).

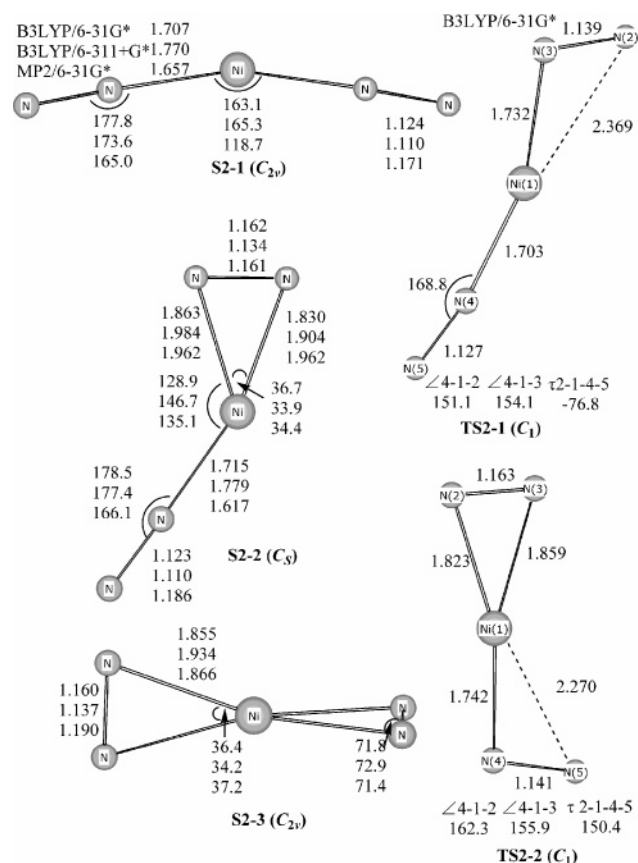


**Figure 2.** Optimized structures for **S2-1** ( $C_{2v}$ ), **S2-2** ( $C_s$ ), **S2-3** ( $C_{2v}$ ), **TS2-a** ( $C_1$ ), and **TS2-b** ( $C_1$ ).

### 3. Results and Discussion

The optimized structures for  $\text{Ni}(\text{N}_2)_x$  ( $x = 1-4$ ) complexes and their corresponding transition states are shown in Figures 1-4, respectively. The total energies, zero-point vibrational energies (ZPVE), single-point energies, and relative energies of the  $\text{Ni}(\text{N}_2)_x$  ( $x = 1-4$ ) complexes are listed in Table 1. The total energies, zero-point vibrational energies of the transition states and the energy differences of the transition states relative to their corresponding  $\text{Ni}(\text{N}_2)_x$  ( $x = 2-4$ ) complexes are listed in Table 2. The harmonic vibrational frequencies and their associated infrared intensities of some  $\text{Ni}(\text{N}_2)_x$  ( $x = 1-4$ ) complexes are listed in Table 3. The dissociation reaction energies for  $\text{Ni}(\text{N}_2)_x$  ( $x = 1-4$ ) complexes performed at the B3LYP/6-311+G\* level of theory are listed in Table 4. A schematic potential energy surface for the isomerization and decomposition reactions of  $\text{Ni}(\text{N}_2)_3$  and  $\text{Ni}(\text{N}_2)_4$  is depicted in Figures 4 and 6, respectively.

**3.1.  $\text{NiN}_2$  Complexes.** As shown in Figure 1, two  $\text{NiN}_2$  complexes, **S1-1** (end-on bound) and **S1-2** (side-on bound), were located as minima at the B3LYP/6-31G\*, B3LYP/6-311+G\*, and MP2/6-31G\* levels of theory. For **S1-2**, the MP2 method predicts similar bond lengths as the DFT does. However, for

**S1-1**, the MP2 method predicts a shorter Ni-N bond length and a longer N-N bond length. This might be attributed to the fact that the MP2 method is, as usual, liable to overestimate the electron correlation effect. Ciullo et al.<sup>7</sup> have performed full optimization on the geometries of both side-on and end-on bound  $\text{NiN}_2$  at the MCPDF level. Their calculated Ni-N and N-N bond lengths are, 1.676 and 1.127 Å for the end-on bound  $\text{NiN}_2$ , and 1.893 and 1.173 Å for the side-on bound one, respectively. Manceron et al.<sup>6</sup> have carried out a DFT study of the end-on bound  $\text{NiN}_2$  and the calculated Ni-N and N-N bond lengths were predicted to be 1.689 and 1.14 Å, respectively. It is obvious that our results at the DFT level are comparable with theirs. From Table 1, it can be seen that the energy of the side-on bound **S1-2** is 10.3 kcal/mol higher than that of the end-on bound **S1-1** at the B3LYP/6-311+G(3df,3pd)//B3LYP/6-311+G\* level including ZPVE at the B3LYP/6-311+G\* level. As seen from Table 4, the dissociation reaction energies including ZPVE corrections for **S1-1** (end-on bound) and **S1-2** (side-on bound) are 11.9 and 0.1 kcal/mol, respectively. Clearly, the end-on coordination is preferred with respect to the side-on one, for which the reason has been explained in the previous study.<sup>7</sup> The nature of the bonding is that **S1-1** (end-on bound) can form two  $\pi$ -back-donative bondings while **S1-2** (side-on bound) can form only one. Moreover, in **S1-1** (end-on bound), the  $\text{N}_2$  can come close to the nickel atom to reach the best overlap.<sup>7</sup>

Combining DFT calculations with matrix-isolation experiments is a powerful approach for studying transition metal complexes. Earlier studies have shown that  $\text{NiN}_2$  is capable of existence in a low-temperature matrix.<sup>2-4</sup> Moreover, by a mixed isotope experiment,<sup>3</sup> the coordination of the obtained  $\text{NiN}_2$  was deduced to be the end-on bound mode rather than the side-on bound one. However, according to the previous theoretical study<sup>6,7</sup> and our DFT calculations, both the end-on and side-on bound  $\text{NiN}_2$  are local minima. What is the reason that the side-on bound  $\text{NiN}_2$  was not detected in the earlier infrared matrix-isolation experiments? From Table 4, we can see that the dissociation reaction energy of **S1-2** (side-on bound) is only 0.1 kcal/mol, which indicates **S1-2** is barely bound with respect to Ni and  $\text{N}_2$ . Therefore, it is inferred that there is no side-on bound  $\text{NiN}_2$  formed in the earlier infrared matrix-isolation experiments.

As shown in Table 3, **S1-1** was calculated to exhibit a strong band at 2249  $\text{cm}^{-1}$  and a weak one at 544  $\text{cm}^{-1}$ , which correspond to the N-N and Ni-N stretching vibrations, respectively. In an earlier infrared matrix-isolation experiment by Klotzbücher and Ozin,<sup>4</sup> the lines at 2089.9 and 466  $\text{cm}^{-1}$  were assigned to the N-N and Ni-N stretches of the end-on bound  $\text{NiN}_2$ , respectively. However, in a recent infrared matrix-isolation study by Manceron et al.,<sup>6</sup> no  $\text{NiN}_2$  band was found at 466  $\text{cm}^{-1}$ . The stretching vibrations of N-N and Ni-N were reassigned at 2089 and 563  $\text{cm}^{-1}$ , respectively. Compared with Manceron's results, our calculated N-N and Ni-N stretching vibrational frequencies are 7.7% higher and 3.3% lower, respectively.

**3.2.  $\text{Ni}(\text{N}_2)_2$  Complexes.** We have explored extensively the potential energy surface of  $\text{Ni}(\text{N}_2)_2$  searching for different structures. Three complexes (**S2-1**, **S2-2**, and **S2-3**) were located as minima at last. Among these three minima, **S2-1** is the most stable one followed by **S2-2** and **S2-3** that are 10.9 and 18.7 kcal/mol higher in energy than **S2-1**, respectively. The initial optimization for **S2-1** was started with a  $D_{\infty h}$  symmetric geometry that has been assigned with two end-on bound  $\text{N}_2$  ligands in an earlier matrix-isolation experiment.<sup>3</sup> However, this

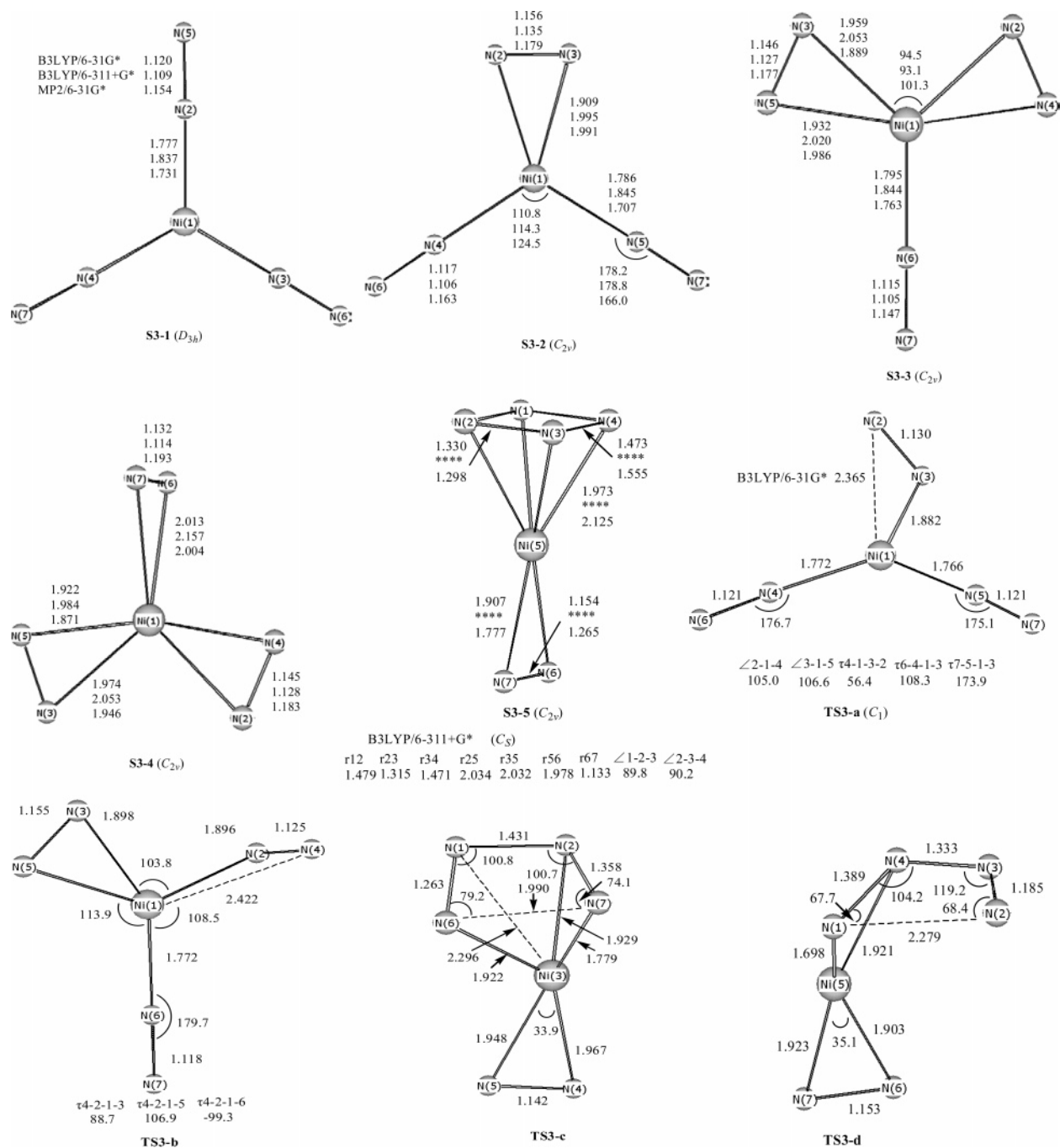


Figure 3. Optimized structures for S3-1 ( $D_{3h}$ ), S3-2 ( $C_{2v}$ ), S3-3 ( $C_{2v}$ ), S3-4 ( $C_{2v}$ ), S3-5 ( $C_{2v}$ ), TS3-a ( $C_1$ ), TS3-b ( $C_1$ ), TS3-c ( $C_1$ ), and TS3-d ( $C_1$ ).

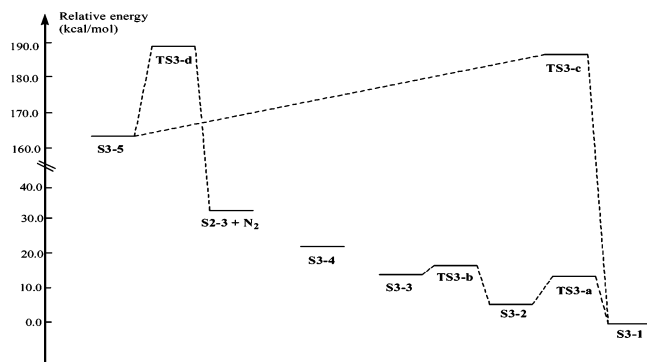


Figure 4. A schematic potential energy surface for the isomerization and decomposition reactions of Ni(N<sub>2</sub>)<sub>3</sub>.

initial geometry turns out to have two small imaginary frequencies at the DFT and MP2 levels with the 6-31G\* basis set, which

may result from a Jahn–Teller distortion. We followed the modes of the imaginary frequencies and ended up with S2-1, a distorted structure with  $C_{2v}$  symmetry. According to the dissociation reaction energies listed in Table 4, it can be seen that there exist strong bond strength in these three Ni(N<sub>2</sub>)<sub>2</sub> complexes.

Two transition states, TS2-a and TS2-b, were found on the potential energy surface of Ni(N<sub>2</sub>)<sub>2</sub>. The IRC calculation confirms that TS2-a is connected to S2-1 and to S2-2 while TS2-b is connected to S2-2 and to S2-3. TS2-a and TS2-b are 8.9 and 11.5 kcal/mol higher in energy than S2-2 and S2-3, respectively, at the B3LYP/6-31G\* level of theory with ZPVE corrections. Such low isomerization barrier heights suggest that S2-2 and S2-3 are not kinetically stable. However, it may be possible to observe them as short-lived species in the matrix-isolation experiment. To assist future experimental detection,

**TABLE 1: Total Energies [au] and Zero-Point Vibrational Energies [kcal/mol] of the Ni(N<sub>2</sub>)<sub>x</sub> (x = 1–4) Complexes Calculated at the MP2/6-31G\*(or B3LYP/6-31G\*), B3LYP/6-311+G\*, and B3LYP/6-311+G(3df,3pd) Levels of Theory, and Single-Point Energies [kcal/mol] and Relative Energies [kcal/mol] at the B3LYP/6-311+G(3df,3pd) Level of Theory**

complexes	MP2/6-31G*	B3LYP/6-31G*	B3LYP/6-311+G*	B3LYP/6-311+G(3df,3pd)	
<b>S1-1</b> ( <i>C<sub>∞v</sub></i> )	−1616.06509 14.0	−1617.56112 4.9	−1617.82667 4.8	−1617.83571	0.0
<b>S1-2</b> ( <i>C<sub>2v</sub></i> )	−1616.07090 21.8	−1617.55713 4.3	−1617.80908 4.0	−1617.81804	10.3 <sup>a</sup>
<b>S2-1</b> ( <i>C<sub>2v</sub></i> )	−1725.43991 11.4	−1727.16862 9.7	−1727.43752 9.7	−1727.45497	0.0
<b>S2-2</b> ( <i>C<sub>s</sub></i> )	−1725.41772 10.6	−1727.16090 9.4	−1727.41843 9.0	−1727.43647	10.9 <sup>a</sup>
<b>S2-3</b> ( <i>C<sub>2v</sub></i> )	−1725.42639 12.3	−1727.16218 9.4	−1727.40477 8.7	−1727.42362	18.7 <sup>a</sup>
<b>S3-1</b> ( <i>D<sub>3h</sub></i> )	−1834.76835 17.1 ( <i>C<sub>s</sub></i> )	−1836.74030 14.5	−1837.00904 14.2	−1837.03413	0.0
<b>S3-2</b> ( <i>C<sub>2v</sub></i> )	−1834.73899 14.5	−1836.73401 14.5	−1836.99824 14.1	−1837.02405	6.2 <sup>a</sup>
<b>S3-3</b> ( <i>C<sub>2v</sub></i> )	−1834.72286 20.5	−1836.71878 14.1	−1836.98106 13.5	−1837.00770	15.9 <sup>a</sup>
<b>S3-4</b> ( <i>C<sub>2v</sub></i> )	−1834.71290 17.0	−1836.70250 13.6	−1836.95933 12.5	−1836.98656	28.2 <sup>a</sup>
<b>S3-5</b> ( <i>C<sub>2v</sub></i> )	−1834.43849 35.8	−1836.48074 14.8	−1836.72183 14.2 ( <i>C<sub>s</sub></i> )	−1836.75332	176.2 <sup>a</sup>
complexes	B3LYP/6-31G*	B3LYP/6-31G*	B3LYP/6-311+G*	B3LYP/6-311+G(3df,3pd)	
<b>S4-1</b> ( <i>T<sub>d</sub></i> )	−1945.86429 19.5	−1946.28445 18.9	−1946.57302 18.5	−1946.60518	0.0
<b>S4-2</b> ( <i>C<sub>s</sub></i> )		−1946.26842 18.5			
<b>S4-3</b> ( <i>D<sub>2</sub></i> )	−1945.81882 18.0	−1946.22067 17.1			
<b>S4-4</b> ( <i>C<sub>2v</sub></i> )	−1945.65848 21.8	−1946.06159 20.6	1946.33177 20.1	−1946.36797	150.5 <sup>a</sup>
<b>S4-5</b> ( <i>C<sub>s</sub></i> )	−1945.63866 21.3	−1946.04280 20.1	−1946.30554 19.2	−1946.34461	164.2 <sup>a</sup>
<b>S4-6</b> ( <i>C<sub>2v</sub></i> )	−1945.61770 20.6	−1946.02279 19.5	−1946.28324 18.4	−1946.32370	176.6 <sup>a</sup>
<b>S4-7</b> ( <i>D<sub>4d</sub></i> )	−1945.39768 23.2	−1945.83111 21.3	−1946.07010 20.9	−1946.11538	309.8 <sup>a</sup>

<sup>a</sup> Single-point energy at the B3LYP/6-311+G(3df,3pd)/B3LYP/6-311+G\* level with ZPVE correction at the B3LYP/6-311+G\* level.

**TABLE 2: Total Energies [au] and Zero-Point Vibrational Energies [kcal/mol] of the Transition States Calculated at the B3LYP/6-31G\* Level of Theory, and Energy Differences of the Transition States Relative to the Ni(N<sub>2</sub>)<sub>x</sub> (x = 2–4) Complexes Calculated at the B3LYP/6-31G\* Level of Theory with ZPVE Corrections**

species	B3LYP/6-31G*	species	B3LYP/6-31G*
<b>S2-3</b> ( <i>C<sub>2v</sub></i> )	−1727.16218 9.4	0.0	<b>S4-7</b> ( <i>D<sub>4d</sub></i> ) −1945.83111 21.3
<b>TS2-b</b> ( <i>C<sub>1</sub></i> )	−1727.14291 8.8	11.5	<b>TS4-f</b> ( <i>C<sub>2</sub></i> ) −1945.68993 17.6
<b>S2-2</b> ( <i>C<sub>s</sub></i> )	−1727.16090 9.4	0.0	<b>TS4-e</b> ( <i>C<sub>1</sub></i> ) −1945.76883 19.3
<b>TS2-a</b> ( <i>C<sub>1</sub></i> )	−1727.14631 9.1	8.9	<b>TS4-d</b> ( <i>C<sub>1</sub></i> ) −1945.75248 18.4
<b>S3-5</b> ( <i>C<sub>2v</sub></i> )	−1836.48074 14.8	0.0	<b>S4-5</b> ( <i>C<sub>s</sub></i> ) −1946.04280 20.1
<b>TS3-d</b> ( <i>C<sub>1</sub></i> )	−1836.43739 13.6	26.0	<b>TS4-c</b> ( <i>C<sub>1</sub></i> ) −1945.98383 17.6
<b>TS3-c</b> ( <i>C<sub>1</sub></i> )	−1836.43904 13.3	24.7	<b>TS4-b</b> ( <i>C<sub>1</sub></i> ) −1946.03442 19.4
<b>S3-3</b> ( <i>C<sub>2v</sub></i> )	−1836.71878 14.1	0.0	<b>S4-4</b> ( <i>C<sub>2v</sub></i> ) −1946.06159 20.6
<b>TS3-b</b> ( <i>C<sub>1</sub></i> )	−1836.71200 13.6	3.8	<b>TS4-a</b> ( <i>C<sub>1</sub></i> ) −1946.00194 18.1
<b>S3-2</b> ( <i>C<sub>2v</sub></i> )	−1836.73401 14.5	0.0	
<b>TS3-a</b> ( <i>C<sub>1</sub></i> )	−1836.71938 13.7	8.4	

the calculated vibrational frequencies of **S2-2** and **S2-3** are provided in Table 3.

Vibrational frequency analysis was performed mainly for the most stable species **S2-1**. According to the study by Klotzbücher and Ozin,<sup>4</sup> the lines at 2106 and 406 cm<sup>−1</sup> were assigned to the N–N and Ni–N stretches of **S2-1**, respectively. In a recent study by Manceron et al.,<sup>6</sup> the band at 469 cm<sup>−1</sup> was found to have an intensity behavior similar to the band at 2106 cm<sup>−1</sup>, which was further confirmed by the photolysis and annealing studies. In contrast with Manceron's results, our calculated N–N and Ni–N stretching vibrational frequencies are 2266 and 507 cm<sup>−1</sup>, respectively, being 7.6% and 8.1% higher than the experimental value.

**3.3. Ni(N<sub>2</sub>)<sub>3</sub> Complexes.** Five structures of Ni(N<sub>2</sub>)<sub>3</sub> were located as minima. **S3-1** (*D<sub>3h</sub>*) is the most stable one that has been previously assigned on the basis of the infrared and Raman absorption intensities.<sup>2,3</sup> It has zero imaginary frequency at the DFT level; however, it has a small imaginary frequency of 9.6*i* at the MP2 level. We followed the mode of the imaginary frequency and ended up with a *C<sub>3v</sub>* symmetric structure, which is only 0.01 kcal/mol lower in energy than the *D<sub>3h</sub>* symmetric one. **S3-2** is the second most stable structure with one side-on and two end-on bound N<sub>2</sub> ligands, being 6.2 kcal/mol higher in energy than **S3-1**. **S3-3** is the third most stable structure with one end-on and two side-on bound N<sub>2</sub> ligands, being 15.9 kcal/mol higher in energy than **S3-1**. Following **S3-3**, **S3-4** has three side-on bound N<sub>2</sub> ligands, being 28.2 kcal/mol less stable than **S3-1**. **S3-5** is the least stable structure with one side-on bound N<sub>2</sub> ligand and one N<sub>4</sub> ligand, being 176.2 kcal/mol higher in

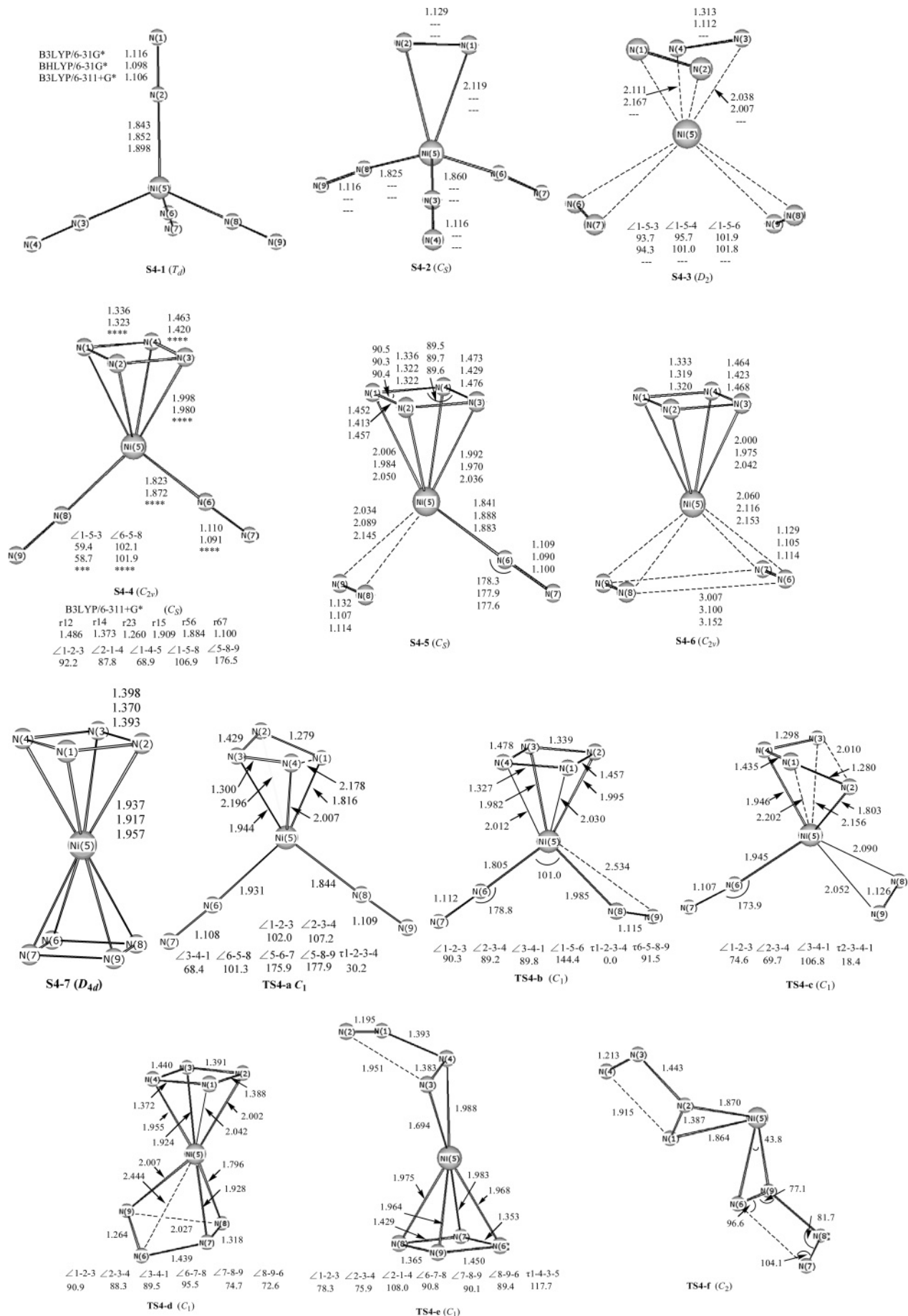


**Figure 5.** Optimized structures for S4-1 ( $T_d$ ), S4-2 ( $C_s$ ), S4-3 ( $D_2$ ), S4-4 ( $C_{2v}$ ), S4-5 ( $C_s$ ), S4-6 ( $C_{2v}$ ), S4-7 ( $D_{4d}$ ), TS4-a ( $C_1$ ), TS4-b ( $C_1$ ), TS4-c ( $C_1$ ), TS4-d ( $C_1$ ), TS4-e ( $C_1$ ), and TS4-f ( $C_2$ ).

**TABLE 3: Harmonic Vibrational Frequencies [ $\text{cm}^{-1}$ ] and Infrared Intensities [ $\text{km/mol}$ ] of Some  $\text{Ni}(\text{N}_2)_x$  ( $x = 1-4$ ) Complexes Calculated at the B3LYP/6-311+G\* Level of Theory<sup>a</sup>**

complexes	(mode) frequency (infrared intensity)
<b>S1-1</b> ( $C_{\infty v}$ )	(PI) 283 (6); (PI) 285 (6); (SG) 544 (17); (SG) 2249 (503)
<b>S1-2</b> ( $C_{2v}$ )	(B <sub>2</sub> ) 334 (9); (A <sub>1</sub> ) 482 (14); (A <sub>1</sub> ) 1993 (221)
<b>S2-1</b> ( $C_{2v}$ )	(A <sub>1</sub> ) 57 (1); (A <sub>2</sub> ) 262 (0); (B <sub>2</sub> ) 265 (0); (B <sub>1</sub> ) 328 (5); (A <sub>1</sub> ) 333 (5); (A <sub>1</sub> ) 427 (0); (B <sub>2</sub> ) 507 (183); (B <sub>2</sub> ) 2266 (1247); (A <sub>1</sub> ) 2319 (6)
<b>S2-2</b> ( $C_s$ )	(A') 66 (2); (A'') 95 (0); (A') 273 (12); (A') 277 (6); (A'') 344 (0); (A'') 392 (7); (A') 475 (123); (A') 2094 (441); (A') 2296 (463)
<b>S2-3</b> ( $C_{2v}$ )	(E) 99 (4); (A <sub>2</sub> ) 193 (0); (B <sub>1</sub> ) 364 (4); (B <sub>2</sub> ) 364 (4); (A <sub>1</sub> ) 365 (0); (A <sub>1</sub> ) 448 (97); (A <sub>1</sub> ) 2083 (510); (A <sub>1</sub> ) 2093 (0);
<b>S3-1</b> ( $D_{3h}$ )	(E') 59 (0); (A <sub>2</sub> ') 65 (1); (E'') 207 (0); (A <sub>2</sub> ') 248 (0); (A <sub>2</sub> ') 336 (0); (E') 339 (112); (A <sub>1</sub> ') 363 (0); (E') 409 (52); (E') 2276 (1666); (A <sub>1</sub> ') 2334 (0)
<b>S4-1</b> ( $T_d$ )	(E) 51 (0); (T <sub>2</sub> ) 64 (0); (T <sub>1</sub> ) 208 (0); (T <sub>2</sub> ) 262 (129); (E) 311 (0); (A <sub>1</sub> ) 323 (0); (T <sub>2</sub> ) 352 (18); (T <sub>2</sub> ) 2301 (1773); (A <sub>1</sub> ) 2361 (0)
<b>S4-4</b> ( $C_s$ )	(A'') 68 (0); (A') 71 (1); (A') 79 (1); (A'') 101 (1); (A') 152 (6); (A'') 271(2); (A'') 291 (2); (A') 326 (1); (A'') 328 (17); (A'') 340 (0); (A') 350 (12); (A'') 395 (2); (A') 501 (16); (A'') 655 (0); (A'') 715 (0); (A') 960 (78); (A'') 1082 (0); (A') 1096 (83); (A') 1509 (73); (A'') 2368 (197); (A') 2389 (171)
<b>S4-7</b> ( $D_{4d}$ )	(B <sub>1</sub> ) 7 (0); (E <sub>1</sub> ) 156 (1); (A <sub>1</sub> ) 357 (0); (E <sub>3</sub> ) 405 (0); (E <sub>1</sub> ) 446 (7); (B <sub>2</sub> ) 600 (46); (E <sub>2</sub> ) 638 (0); (E <sub>2</sub> ) 922 (0); (E <sub>1</sub> ) 943 (1); (E <sub>3</sub> ) 955 (0); (E <sub>2</sub> ) 1155 (0); (A <sub>1</sub> ) 1199 (0); (B <sub>2</sub> ) 1203 (0.4)

<sup>a</sup> The intensities of degenerate modes have been doubled or trebled.

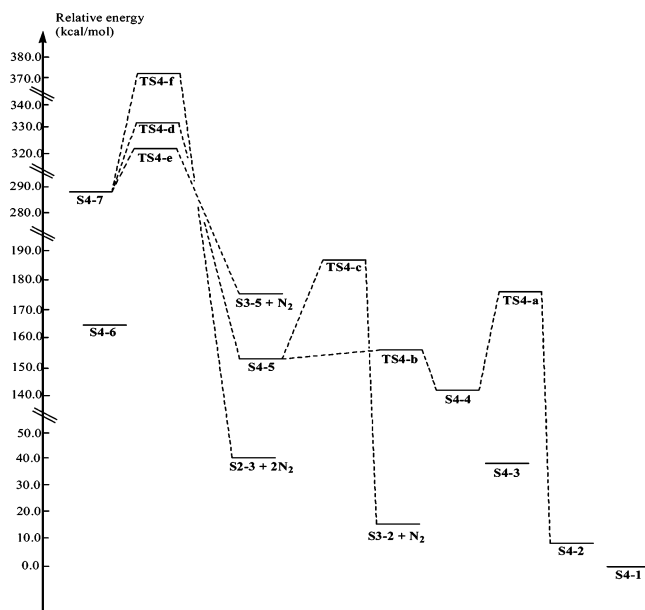
**TABLE 4: Dissociation Reaction Energies with ZPVE Corrections Calculated at the B3LYP/6-311+G\* Level of Theory [kcal/mol]<sup>a</sup>**

reactions	<i>E</i>	reactions	<i>E</i>
<b>S1-1</b> → Ni + N <sub>2</sub>	11.9	<b>S4-1</b> → <b>S3-1</b> + N <sub>2</sub>	3.5
<b>S1-2</b> → Ni + N <sub>2</sub>	0.1	<b>S4-1</b> → Ni + 4N <sub>2</sub>	43.1 (10.8)
<b>S2-1</b> → <b>S1-2</b> + N <sub>2</sub>	33.5	<b>S4-2</b> → <b>S3-1</b> + N <sub>2</sub>	-19.3
<b>S2-1</b> → Ni + 2N <sub>2</sub>	45.4 (22.7)	<b>S4-3</b> → <b>S3-4</b> + N <sub>2</sub>	-186.1
<b>S2-2</b> → <b>S1-1</b> + N <sub>2</sub>	20.8	<b>S4-4</b> → <b>S2-1</b> + N <sub>4</sub>	42.7
<b>S2-2</b> → <b>S1-2</b> + N <sub>2</sub>	32.7	<b>S4-5</b> → <b>S2-2</b> + N <sub>4</sub>	38.1
<b>S2-3</b> → <b>S1-2</b> + N <sub>2</sub>	23.7	<b>S4-5</b> → <b>S3-5</b> + N <sub>2</sub>	16.6
<b>S2-3</b> → Ni + 2N <sub>2</sub>	23.9 (12.0)	<b>S4-6</b> → <b>S2-3</b> + N <sub>4</sub>	32.1
<b>S3-1</b> → <b>S2-1</b> + N <sub>2</sub>	8.4	<b>S4-7</b> → Ni + 2N <sub>4</sub>	105.4 (52.7)
<b>S3-1</b> → Ni + 3N <sub>2</sub>	21.9 (7.3)		
<b>S3-2</b> → <b>S2-2</b> + N <sub>2</sub>	14.2		
<b>S3-3</b> → <b>S2-3</b> + N <sub>2</sub>	11.7		
<b>S3-4</b> → <b>S2-3</b> + N <sub>2</sub>	-2.9		
<b>S3-5</b> → <b>S1-2</b> + N <sub>4</sub>	54.1		

<sup>a</sup> The mean dissociation reaction energies are listed in the parentheses.

energy than **S3-1**. For **S3-5**, the N<sub>4</sub> ligand can be regarded as a complex composed of two side-on bound N<sub>2</sub> ligands. As seen from Table 4, all Ni(N<sub>2</sub>)<sub>3</sub> complexes are well bound except for **S3-4**, of which the dissociation reaction energy is -2.9 kcal/mol.

Four transition states (**TS3-a**, **TS3-b**, **TS3-c**, and **TS3-d**) were found on the potential energy surface of Ni(N<sub>2</sub>)<sub>3</sub>. **TS3-a** is a transition state of the isomerization from **S3-2** into **S3-1**. The barrier height is 8.4 kcal/mol at the B3LYP/6-31G\* level of theory with ZPVE correction. **TS3-b** is a transition state of the isomerization reaction from **S3-3** into **S3-2** with a barrier height of 3.8 kcal/mol. **TS3-c** is a transition state of the isomerization reaction from **S3-5** into **S3-1** with a barrier height of 24.7 kcal/mol. **TS3-d** is a transition state of the dissociation reaction of **S3-5** into Ni(N<sub>2</sub>)<sub>2</sub> (**S2-3**) and N<sub>2</sub>. The dissociation barrier height is 26.0 kcal/mol. For each molecule, it can isomerize and/or decompose easily along the pathway of which the barrier height

**Figure 6.** A schematic potential energy surface for the isomerization and decomposition reactions of Ni(N<sub>2</sub>)<sub>4</sub>.

is below 30 kcal/mol. From the results presented here, it seems that the Ni(N<sub>2</sub>)<sub>3</sub> complexes are not kinetically stable enough.

According to the experiment by Klotzbücher and Ozin,<sup>4</sup> the lines at 2134 and 343 cm<sup>-1</sup> belong to the N-N and Ni-N stretching vibrations of **S3-1**. In the present study, the calculated N-N and Ni-N stretching vibrational frequencies for **S3-1** are 2276 and 339 cm<sup>-1</sup>, respectively, which are 6.7% higher and 1.2% lower than the experimental value.

**3.4. Ni(N<sub>2</sub>)<sub>4</sub> Complexes.** Previous experiment<sup>2</sup> has shown that Ni(N<sub>2</sub>)<sub>4</sub> in argon is a regular tetrahedral molecule with end-on bound dinitrogen; however, it is slightly distorted in pure nitrogen. Following this study, we optimized the *T<sub>d</sub>* symmetric Ni(N<sub>2</sub>)<sub>4</sub> (**S4-1**), and proved it to be the most stable minimum at the DFT level of theory. We have optimized six other structures of the Ni(N<sub>2</sub>)<sub>4</sub>: **S4-2** (formed from one side-on and three end-on bound N<sub>2</sub> ligands), **S4-3** (from four side-on bound N<sub>2</sub> ligands), **S4-4** (from one N<sub>4</sub> ligand and two end-on bound N<sub>2</sub> ligands), **S4-5** (from one N<sub>4</sub> ligand, one end-on bound N<sub>2</sub> ligand, and one side-on bound N<sub>2</sub> ligand), **S4-6** (from one N<sub>4</sub> ligand and two side-on bound N<sub>2</sub> ligands), and **S4-7** (from two N<sub>4</sub> ligands). **S4-7** have recently been reported to be a possible high-energy species.<sup>17</sup> It can be regarded either as a complex of a neutral 4π-electron N<sub>4</sub> with a metal atom or, at the ionic limit, as a complex of a 6π-electron N<sub>4</sub><sup>2-</sup> anion and a Ni<sup>4+</sup> cation. The latter presumption seems more reasonable than the former one because all N-N bond lengths are equal and the calculated Wiberg bond indices (WBI) are the same, 1.2, which indicates a complete delocalization of the N<sub>4</sub> ring. For **S4-4**, **S4-5**, and **S4-6**, the N<sub>4</sub> ligand can be regarded as a complex of two side-on bound N<sub>2</sub> ligands with 4π-electrons. It is obvious that the potential energy surface becomes more complex when the number of ligands increases. Furthermore, according to the relative energy analyses for all Ni(N<sub>2</sub>)<sub>x</sub> ( $x = 1-4$ ) complexes, it is found that the end-on bound complexes are the most stable species followed by the side-on bound and N<sub>4</sub>-ligand bound ones.

From Table 4, it can be seen that the mean dissociation reaction energies of **S1-1** → Ni + N<sub>2</sub>, **S2-1** → Ni + 2N<sub>2</sub>, **S3-1** → Ni + 3N<sub>2</sub>, and **S4-1** → Ni + 4N<sub>2</sub> are 11.9, 22.7, 7.3, and 10.8 kcal/mol per N<sub>2</sub>, respectively, which indicates that **S2-1** is the best bound structure while **S3-1** is the worst bound one.

The dissociation reaction energies of **S4-2** and **S4-3** are both negative, suggesting that the existence of **S4-2** and **S4-3** in a matrix-isolation experiment is impossible. The dissociation reaction energies of **S3-5** → **S1-2** + N<sub>4</sub>, **S4-4** → **S2-1** + N<sub>4</sub>, **S4-6** → **S2-3** + N<sub>4</sub>, and **S4-7** → Ni + 2N<sub>4</sub> suggest that N<sub>4</sub> can bind well with the Ni atom.

On the PES of Ni(N<sub>2</sub>)<sub>4</sub>, several decomposition and isomerization reactions were investigated at the B3LYP/6-31G\* level of theory. **TS4-a** is a transition state of the isomerization reaction from **S4-4** into **S4-2**. The barrier height of 34.9 kcal/mol suggests that **S4-4** may be kinetically stable. **TS4-c** is a transition state of the decomposition reaction of **S4-5** into Ni(N<sub>2</sub>)<sub>3</sub> (**S3-2**) and one N<sub>2</sub> molecule. The decomposition barrier height of 34.5 kcal/mol indicates that **S4-5** is difficult to decompose. However, a transition state **TS4-b** was found for the isomerization reaction from **S4-5** into **S4-4** with a barrier height of only 4.6 kcal/mol. In a word, **S4-5** is not kinetically stable and will isomerize into **S4-4** easily. **TS4-d** is a transition state of the isomerization reaction from **S4-7** into **S4-5** with a barrier height of 46.4 kcal/mol. Several decomposition reactions of **S4-7** have recently been predicted by us.<sup>17</sup> **TS4-e** is a transition state corresponding to the decomposition reaction of **S4-7** into Ni(N<sub>2</sub>)<sub>3</sub> (**S3-5**) and one N<sub>2</sub> molecule, while **TS4-f** is a transition state corresponding to the decomposition reaction of **S4-7** into Ni(N<sub>2</sub>)<sub>2</sub> (**S2-3**) and two N<sub>2</sub> molecules. The decomposition barrier heights are 37.1 and 84.9 kcal/mol, respectively. Such high isomerization and decomposition barriers indicate that **S4-7** is likely to be kinetically stable enough to resist both isomerization and decomposition. According to the present studies on the isomerization and decomposition reactions of Ni(N<sub>2</sub>)<sub>x</sub> (x = 2–4), it is suggested that the side-on bound N<sub>2</sub> ligand is easy to transform into the end-on bound one; however, the N<sub>4</sub> bound ligand is hard to transform into either the side-on or the end-on bound N<sub>2</sub> ligand.

In an earlier study by Klotzbücher and Ozin,<sup>4</sup> the experimental N–N and Ni–N stretching vibrational frequencies for **S4-1** are 2175 and 282 cm<sup>-1</sup>, respectively. In the present study, harmonic vibrational frequency analyses were carried out mainly for **S4-1**, **S4-4**, and **S4-7**. For **S4-1**, the calculated harmonic vibrational frequencies are 2301 and 262 cm<sup>-1</sup> corresponding to the N–N and Ni–N stretches, respectively, which are 5.8% higher and 7.1% lower than the experimental value. From the above contrast for **S1-1**, **S2-1**, **S3-1**, and **S4-1**, the discrepancy between the calculation results and the experimental value is in the range of 1.2–8.1%. This discrepancy may be due to the matrix effects and/or the systematic errors in the DFT method (of which the error is usually about 0.05). For **S4-4**, the calculated harmonic vibrational frequencies are 960, 1509, 2368, and 2389 cm<sup>-1</sup> corresponding to the N1–N2 (N3–N4), N1–N4 (N2–N3), and N6–N7 (N8–N9) symmetric, and N6–N7 (N8–N9) asymmetric stretches, respectively. For **S4-7**, the calculated harmonic vibrational frequency is 600 cm<sup>-1</sup> corresponding to the N<sub>4</sub>–Ni–N<sub>4</sub> stretch.

#### 4. Summary

The geometries of 17 Ni(N<sub>2</sub>)<sub>x</sub> (x = 1–4) complexes were fully optimized at the B3LYP/6-31G\* and MP2/6-31G\* levels of theory (for Ni(N<sub>2</sub>)<sub>x</sub> (x = 4), the MP2 method was substituted

with the B3LYP method). Harmonic vibrational frequencies were calculated at the same level of theory. Structures for all complexes were further optimized at the B3LYP/6-311+G\* level of theory followed by single-point energy calculation at the B3LYP/6-311+G(3df,3pd) level of theory. The decomposition and isomerization pathways of the Ni(N<sub>2</sub>)<sub>x</sub> (x = 2–4) complexes were studied at the B3LYP/6-31G\* level of theory, and 12 transition states were found. The intrinsic reaction coordinate calculations performed at the same level confirm that these 12 transition states connect the right complexes. Energy analyses suggest that end-on bound Ni(N<sub>2</sub>)<sub>x</sub> (x = 1–4) complexes are preferred to side-on and N<sub>4</sub> (which can be considered as a complex of two side-on bound N<sub>2</sub>) bound ones. The present study shows that except for the four assigned complexes (NiN<sub>2</sub> (C<sub>∞v</sub>), Ni(N<sub>2</sub>)<sub>2</sub> (D<sub>∞h</sub>), Ni(N<sub>2</sub>)<sub>3</sub> (D<sub>3h</sub>), and Ni(N<sub>2</sub>)<sub>4</sub> (T<sub>d</sub>)), another two complexes (Ni(N<sub>2</sub>)<sub>4</sub> (C<sub>2v</sub>) and Ni(N<sub>2</sub>)<sub>4</sub> (D<sub>4d</sub>)) may be kinetically stable. The calculated bond lengths and harmonic vibrational frequencies may assist future laboratory identification of these two possible complexes. Although another 11 complexes were also identified as energy minima on the potential energy surfaces, they are not kinetically stable toward isomerization into more stable complexes. The present study also suggests that the side-on bound N<sub>2</sub> ligand is ready to transform into the end-on bound one, while the N<sub>4</sub> ligand is hard to transform into either the side-on or the end-on bound N<sub>2</sub> ligand.

#### References and Notes

- (1) Collman, J. P.; Hegedus, L. S.; Norton, J. R.; Finke, R. G. *Principles and Applications of Organotransition Metal Chemistry*; University Science Books: Mill Valley, CA, 1987.
- (2) Burdett, J. K.; Turner, J. J. *Chem. Commun.* **1971**, 885.
- (3) Huber, H.; Kündig, E. P.; Moskovits, M.; Ozin, G. A. *J. Am. Chem. Soc.* **1973**, *95*, 332.
- (4) Klotzbücher, W.; Ozin, G. A. *J. Am. Chem. Soc.* **1975**, *97*, 2672.
- (5) Bauschlicher, C. W., Jr.; Langhoff, S. R.; Barnes, L. A. *Chem. Phys.* **1989**, *129*, 431.
- (6) Manceron, L.; Alikhani, M. E.; Joly, H. A. *Chem. Phys.* **1998**, *228*, 73.
- (7) Ciullo, G.; Rosi, A.; Sgamellotti, A.; Floriani, C. *Chem. Phys. Lett.* **1991**, *185*, 522.
- (8) Moskovits, M.; Ozin, G. A. *J. Chem. Phys.* **1973**, *58*, 1251.
- (9) Siegbahn, P. E. M.; Blomberg, M. R. A. *Chem. Phys.* **1984**, *87*, 189.
- (10) Kao, C. M.; Messmer, R. P. *Phys. Rev. B* **1985**, *31*, 4835.
- (11) Bauschlicher, C. W., Jr. *Chem. Phys. Lett.* **1985**, *115*, 387.
- (12) Siegbahn, P. E. M. *J. Chem. Phys.* **1991**, *95*, 364.
- (13) Khan, F. A.; Steele, D. L.; Armentrout, P. B. *J. Phys. Chem.* **1995**, *99*, 7819.
- (14) Duarte, H. A.; Salahub, D. R.; Haslett, T.; Moskovits, M. *Inorg. Chem.* **1999**, *38*, 3895.
- (15) Haslett, T. L.; Fedrigo, S.; Bosnick, K.; Moskovits, M.; Duarte, H. A.; Salahub, D. *J. Am. Chem. Soc.* **2000**, *122*, 6039.
- (16) Frisch, M. J.; Trucks, G. W.; Schlegel, H. B.; Scuseria, G. E.; Robb, M. A.; Cheeseman, J. R.; Zakrzewski, V. G.; Montgomery, J. A., Jr.; Stratmann, R. E.; Burant, J. C.; Dapprich, S.; Millam, J. M.; Daniels, A. D.; Kudin, K. N.; Strain, M. C.; Farkas, O.; Tomasi, J.; Barone, V.; Cossi, M.; Cammi, R.; Mennucci, B.; Pomelli, C.; Adamo, C.; Clifford, S.; Ochterski, J.; Petersson, G. A.; Ayala, P. Y.; Cui, Q.; Morokuma, K.; Malick, D. K.; Rabuck, A. D.; Raghavachari, K.; Foresman, J. B.; Cioslowski, J.; Ortiz, J. V.; Baboul, A. G.; Stefanov, B. B.; Liu, G.; Liashenko, A.; Piskorz, P.; Komaromi, I.; Gomperts, R.; Martin, R. L.; Fox, D. J.; Keith, T.; Al-Laham, M. A.; Peng, C. Y.; Nanayakkara, A.; Challacombe, M.; Gill, P. M. W.; Johnson, B.; Chen, W.; Wong, M. W.; Andres, J. L.; Gonzalez, C.; Head-Gordon, M.; Replogle, E. S.; Pople, J. A. *Gaussian 98*; Gaussian, Inc.: Pittsburgh, PA, 1998.
- (17) Li, Q. S.; Guan, J. *J. Phys. Chem. A*, **2003**, *107*, 8584–8593.